Applied Mathematical Sciences, Vol. 13, 2019, no. 17, 833 - 843
HIKARI Ltd, www.m-hikari.com
https://doi.org/10.12988/ams.2019.98111

Impact of Sputtering Yield and Backscattered Ion Coefficient on Plasma Facing Surface Exposed to Energetic Charged Particles in the Fusion Reactor

R. Moultif, A. Dezairi, O. Elhaitamy, L. Salama, M. El Marsi, S. Rochd and K. Elghazaouy

Condensed Matter Physics Laboratory, Faculty of Science
Ben M'sik, Hassan II University of Casablanca, Morocco

Abstract

The impact of plasma charged particles on material surfaces relates to several different fundamental processes, such as physical sputtering of material surface bombarded by energetic ions, the reflection of ions from the surface, and ion implantation and re-emission. Among these processes, physical sputtering yield and backscattered ions coefficient may be the most important in determining the performance and life time of plasma wall components.

In this paper, we have applied the Monte Carlo simulation program SRIM to calculate sputtering yield and backscattered ion coefficient of surface plasma facing components (tungsten W, carbon C, beryllium Be) exposed to energetic charged particles in International Thermonuclear Experimental Reactor (ITER). The calculations are significant for the optimization of material facing plasma in future fusion reactors where erosion and long term operation are key issues.

Keywords: Sputtering yield, Backscattered ion coefficient, Plasma facing component**,** Monte Carlo code SRIM

I- Introduction

The damaging effects of energetic charged particles on material surfaces in fusion devices are one of the most important issues in determining fusion plasma performance and lifetime of plasma-facing components (PFC) in fusion reactors [1].

The performance of the plasma facing components (PFC) and materials in fusion reactor are fundamental issues affecting the ultimate technological and economic feasibility of fusion power [2-3]. Many factors influence the choice of a functional and structural material in fusion reactor. The optimization of the wall material is done mainly based on the heat lead capacity in the divertor region, material erosion due to main plasma exposure, fuel retention and surface emission of the secondary ions and the electrons, which significantly influence the plasma wall interaction [4].

The wall materials especially limiter and divertor plates, have to fulfill several criteria: high thermal conductivity for removing the deposited energy, high melting point and large thermal shock resistance, low erosion under plasma bombardment to reduce plasma contamination and excessive thinning of the wall, a favorable behavior with respect to trapping and release of hydrogen to allow good plasma density control and a low long term tritium inventory. Further, the wall material must withstand the large 14 Mev neutron fluxes with only tolerable degradation of its thermo-mechanical properties. Finally, the material should allow good machining and brazing properties to the coolant structure.

Physical sputtering of first- wall materials by energetic plasma particles is expected to be a major source of plasma contamination in fusion power reactors.

The sputtering phenomenon was discovered early last century but was not formulated theoretically until 1969, when Thompson and Sigmund [4]are proposed the sputtering model based on the binary collision cascade concept. Physical sputtering is a consequence of energy and momentum transfer between the incident ions and the surface atoms, due to collision cascades [5,6]. It is quantified by the sputtering yield, i.e. the mean number of atoms removed per incident particle depends on the ion incident angle, the ion incident energy, the masses of the ion and target atoms, the surface binding energy, but it is independent of the charge [7]. The physical sputtering process in fusion devices is due to energetic ions or atoms that escape from the scrape of the layer and impinge on the material surface, undergoing a series of classic collisions and depositing a fraction of their kinetic energies to atoms in the plasma face components surface [8,9]. As a result both the incident particles and the energetic recoil atoms can be scattered back toward the surface. If their kinetic energies are high enough to overcome the surface potential barrier, they can leave the surface and influx to the fusion plasma. This is the so-called sputtering process.

A surface atom is ejected if the cascade of atoms reaches the surface with an energy larger than the surface binding energy [10,11,12]. The threshold energy E_{th} is defined as the minimum ionic energy required below which the sputtering yield is zero [13].

It is known that the Monte Carlo method is a very feasible way to simulate the trajectory of the incident ion and the damage produced by that ion in materials based on the binary collision approximation model [14]. The SRIM (formerly TRIM) is a software package named as the stopping and Range of Ions in Matter, which calculate many features of the transport of ions in matter, such as sputtering yield, implantation, target damage and backscattering [15]. It is based on

Sigmund's theory of physical sputtering this program considers only binary collisions with target atoms initially at rest.

In this research, the Monte Carlo simulation program SRIM was employed to calculate the sputtering yield and backscattered ion coefficient of three candidate plasma face component (PFC) materials (Tungsten W, Beryllium Be, and Carbon C) by energetic H^+, D^+, T^+ and He^+ ion bombardment.

The result are particularly important for estimating the lifetime of plasma face component (PFC) and analyzing the extent of impurity contamination, especially for high-power density and with a high plasma current fusion reactor.

II- Analytical model of sputtering

In 1984, Bohdansky [2] has introduced the most widely analytical formula for calculating sputtering yields. This formula is based on Sigmund's analytic sputtering theory[14], describes the sputtering yield as a function of the projectile energy at a normal incidence.

$$Y(E_0, \alpha = 0^\circ) = Q S_n^{TF}(\varepsilon)\left(1 - \left(\frac{E_{th}}{E_0}\right)^{2/3}\right)\left(1 - \frac{E_{th}}{E_0}\right)^2 \qquad (1)$$

The values Q and E_{th} in Eq.(1) are used as parameters to fit the sputtering data.
Q Determines the maximum of the yield curve, and E_{th} is the threshold energy where the sputtering yield becomes zero.
E_0Is the projectile energy, α is the angle of incidence. $S_n^{TF}(\varepsilon)$ the nuclear stopping cross section and ε the reduced energy [16].

$$\varepsilon = E_0 \frac{M_2}{M_1+M_2}\frac{a_L}{Z_1 Z_2 e^2} = \frac{E_0}{E_{TF}} \qquad \text{with} \qquad E_{TF} = \frac{Z_1 Z_2 e^2}{a_L}\frac{M_1+M_2}{M_2} \qquad (2)$$

Z_1 and Z_2 are the nuclear charges and $M_1$and M_2 the masses of the projectile and the target atom, respectively, e is the electron charge. The Lindhard screening length a_L is given by

$$a_L = \left(\frac{9\pi^2}{128}\right) a_B \left(Z_1^{2/3} + Z_2^{2/3}\right)^{-1/2} = 0{,}4685\ \left(Z_1^{2/3} + Z_2^{2/3}\right)^{-1/2}\ \text{Å} \qquad (3)$$

a_B Is the Bohr radius.
The energy E_{TF} can be written

$$E_{TF}(eV) = 30{,}74\ \frac{M_1+M_2}{M_2} Z_1 Z_2\ \left(Z_1^{2/3} + Z_2^{2/3}\right)^{1/2} \qquad (4)$$

For the dependence of the sputtering yield on the angle of incidence of the bombarding particles, Yamamura proposed a procedure which is based on the

assumption that the angular dependence can be described by a factor to the yield at normal incidence.

$$Y(E_0,\alpha) = Y(E_0,\alpha = 0^{\circ})(\cos\alpha)^{-1}\exp(f(1-(cos\alpha)^{-1})cos\alpha_{opt}) \quad (5)$$

Sigmund [7] proposes the term$(\cos\alpha)^{-1}$, the value f and α_{opt} are usedas fitting parameters.

III- Calculations details

In this paper, we have used the Monte Carlo simulation program SRIM that uses the binary collision approximation (BCA), applied to ion-solid interactions (proposed by J. F. Zeigler and J.P. Biersack) [17] to calculate the sputtering yield and backscattered ion coefficient of three candidate plasma face components (PFC) materials (tungsten W, beryllium Be, carbon C) by energetic $H^+, D^+, T^+ and\ He^+$ion bombardment. These calculations are made in two different cases, when the ions are 60°, and also for different angles of incidence on the (PFC) materials in the energy range 0-10 KeV.
The input parameters used in calculating the sputtering yields and backscatteredion coefficient (%) of tungsten W, beryllium Be and carbon C for SRIM simulation are summarized below:

Table 1. Parameters input used in calculating the sputtering yield and backscattering fraction (%) of PFC materials.

Plasma face components (PFC)	Surface binding energy (eV)	Displacement energy (eV)	Lattice binding energy (eV)	Density $(^{g}/_{cm^3})$
Tungsten (W)	8,68	25	3	19,35
Carbon (C)	7,45	28	3	2,253
Beryllium (Be)	3,38	25	3	1,848

In table 1.we report the SRIM has a built-in compound dictionary, which contains the three PFC materials such as W,C and Be respectively. These materials are characterized by a predefined surface binding energy E_s(8,68 ; 7,45 and 3,38 eV respectively), displacement energy $E_{disp}(25\ ;\ 28\ and\ 25\ eV$ respectively).

IV- Results

First we notice in fig. 1 sputtering yield of carbon target for the various ions species as a function of ion energy at an angle of incidence of 60°, we note here that the sputtering yield in the case of He ion is greater by comparing it to the sputtering yield in the case of the H, D, and T. We see that the sputtering threshold energy of carbon is $E_{th} = 60\ eV$, and the sputtering yield is increased when the ion energy is about $0\ KeV$ to $1\ KeV$, and is decreased when the ion energy is about 1,5 KeV to 10KeV.

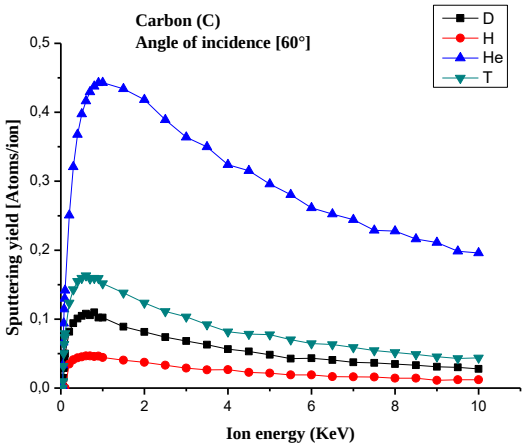

Figure 1: Calculated sputtering yields of Carbon target for various ions species as a function of ion energy at an angle of incidence of 60°

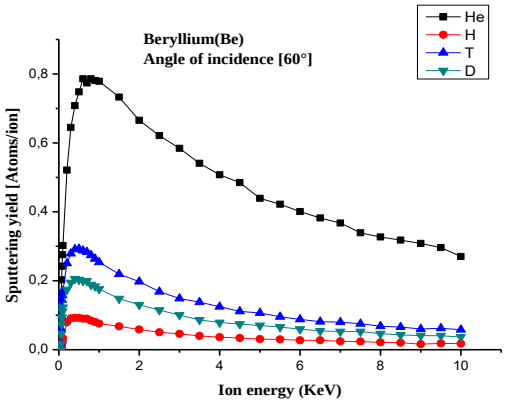

Figure 2: Calculated sputtering of Beryllium (Be) target for various ion species as a function of ion energy at an angle of incidence 60°

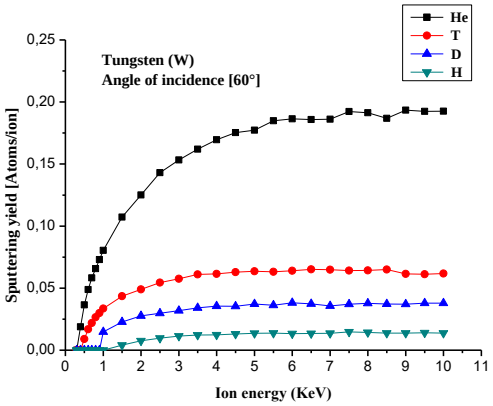

Figure 3: Calculated sputtering yield of tungsten *W* target for various ion species as a function of ion energy at an angle of incidence of 60°.

Concerning the fig.2, it illustrates the sputtering yield of Be target for various ions species as function of ion energy at an angle of incidence of 60°, We note here that the sputtering yield in the case of He ion is greater by comparing it to the sputtering yield in the case of the H, D and T; We see that the sputtering threshold energy of Be is $E_{th} = 30\ eV$, and the sputtering yield is increased when the ion energy is about $0\ KeV$to $0{,}8\ KeV$, and is decreased when the ion energy is about $1KeV$ to $10\ KeV$.

Second, we see in fig. 3 sputtering of tungsten W target by various ion species as function as ion energy at an angle of incidence of 60°. We show two different regimes, initially for an energy of the incident ion lower than $5{,}5\ KeV$, the sputtering yield increases with ions incident energy until reaching a maximum value, but for ions energy range ($5{,}5$ – $10\ KeV$)the sputtering yield becomes stable. The sputtering threshold energy of tungsten W is $E_{th} = 500\ eV$.

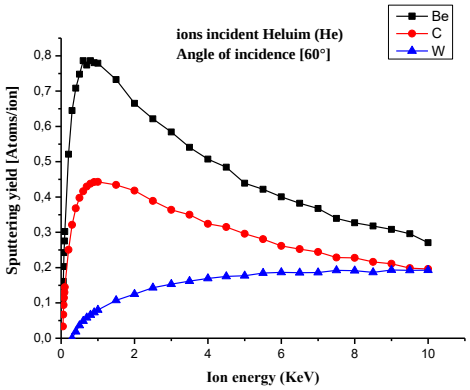

Figure 4. The calculated sputtering yield of candidate first-wall materials ($W, C$and Be) bombarded with monoenergetic helium ions at an angle of incidence of 60°.

The fig.4 treats the sputtering yields for W, Be and C target when bombarded with Helium (He) ions at an angle of incidence of 60°, we note here that the beryllium has the lowest atomic number of any structural material, carbon is a low Z material of much interest and tungsten, although a high Z material, has one of the lowest sputter yields of candidate first-wall materials. These curves, although similar in shape have somewhat flatter peaks. Also the sputtering yield is increased when the ion energy in the energy range (0 - 0,9KeV), and is decreased in the energy range (1 - 10 KeV).

In the figure 5, we note that the angular dependence of sputtering yield represents one of the important characteristics of sputtering at normal ion incidence on the target (i,e. it is equal to 0°), sputtering yield takes its minimum value. With increasing incidence angle sputtering yield increases and at some value 80° achieves its maximum. With the further increase of the angle 80° sputtering yield decreases. Though of the sputtering yield of Beryllium (Be) is

greater by comparing from the sputtering yield of the C and W. The maximum value of the normalized sputtering yield of W is about 0,1 while the same value for C is about 0,8 and the same value of Be is about 1,5 curves might be somewhat high. Anyhow, it is clear that the (W, C and Be) sputtering yields versus the angle of incidence curves strongly deviate, which results in a strong dependence of the relative sputtering yield on the angle of incidence.

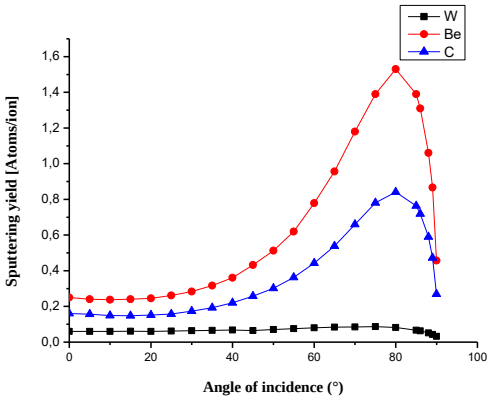

Figure 5 : The calculated sputtering yield of the various targets (W, C and Be) under He ion bombardment as a function of the angle of incidence for at an ion energy of $1KeV$.

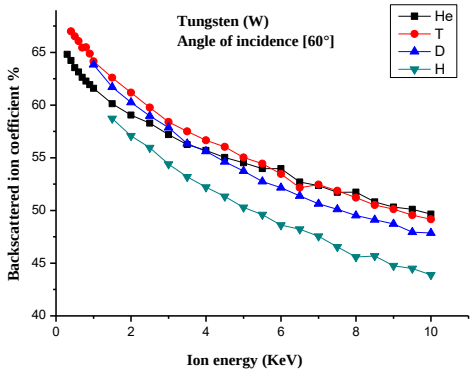

Figure 6: The backscattered ion coefficient for tungsten (W) versus the ion primary energy of H, D, T and He at an incidence angle of 60°

Figure 6 depicts the relationship between the backscattered ion coefficient and the incident energy for different ions H, D, T and He. So the backscattering ion coefficient for tungsten at an incidence angle of 60° is a decreasing function of the primary ion energy.

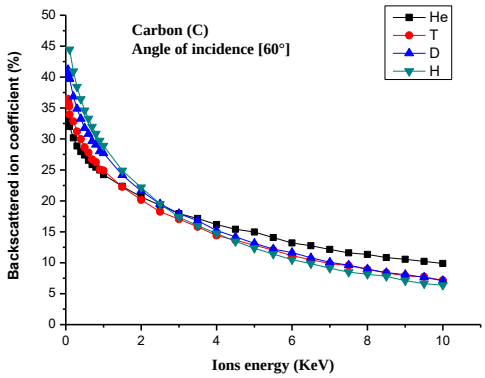

Figure 7: The backscattered ion coefficient for carbon (C) versus the ion primary energy of H, D, T and He at an incidence angle of 60°

This figure treats the backscattered ion coefficient for carbon at an incidence angle of 60°, it is clearly seen from these data that the backscattered ion coefficient for carbon target decreases with increasing of ions energy .

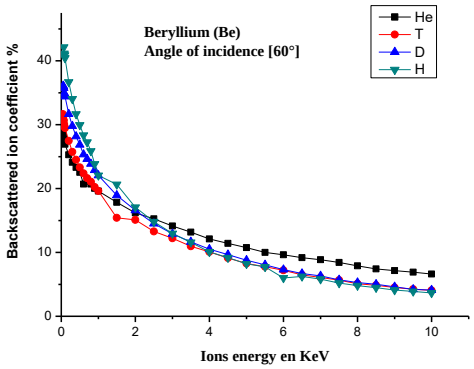

Figure 8 :The backscattered ion coefficient for beryllium (Be) versus the ion primary energy of H, D, T and He at an incidence angle of 60°

The fig. 8 treats the backscattered ion coefficient for beryllium (Be) versus the ion primary energy of H, D, T and He at an incidence angle of 60°, we note here that the backscattered ion coefficient decreases with increasing of ion energy. On the other hand, for high-energy value of backscattered ions coefficient becomes low.

In addition the fig. 9 shows The backscattered Helium (He) coefficient for various targets (W, C, Be) versus the ion primary energy of Heat an incidence angle of 60°. Here, we observe that the curves have the same shape on the increase of the backscattering factor while increasing the energy, the backscattered ion coefficient of tungsten W is higher compared with the C and Be backscattered ion. So a higher atomic number Z target (W) gives higher values of

backscattered ion coefficient than low atomic number Z target. The backscattered ion coefficient increases as the atomic number Z increases.

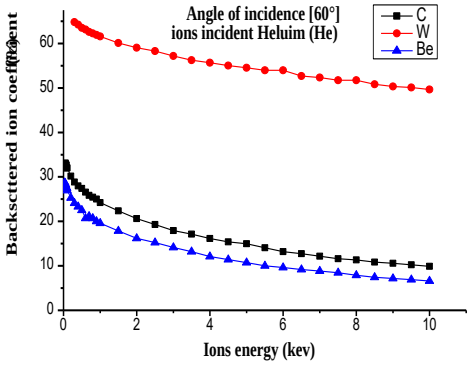

Figure 9 : The backscattered Helium (He) coefficient for various targets (W, C, Be) versus the ion primary energy of He at an incidence angle of 60°

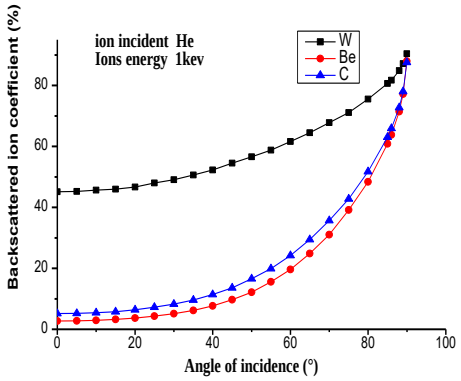

Figure 10: Backscattered ion coefficient versus angle of incidence from various targets (W, C and Be)

Furthermore, fig 10 shows the backscattered ion coefficient of the ion He according to its angle of incidence. We observe that the curves have the same shape on the increase of the backscattered ion coefficient, while increasing the angle of incidence. Anyhow, it is clear that the backscattered ion coefficient have a strong dependence of the angle of incidence.

V- Conclusion

Despite all the work done on the improvement of plasma confinement, it will never be perfect. Plasma-facing components in every fusion device are exposed to high heat and particle fluxes from plasma. This makes the development of PFCs is one of the key issues in fusion science and technology.

In this study, we have calculated by Monte Carlo simulation program SRIM the sputtering yields and backscattered ions coefficient for energetic (He, D, T, H) as function as ion bombardment of three candidate plasma face component (W, C,

Be). Results show that the sputtering yield and backscattered ions coefficient have a strong dependence on the target mass, projectile energy, and angle of incidence. Comparison between three-candidate face material we find that the tungsten W component has a low sputtering yield, a high backscattered ions coefficient and has a high threshold energy.

Therefore, the tungsten is a good choice for the plasma face component and a prime candidate to be used in future fusion reactors.

References

[1] Shimomura, Y. Aymar, R. Chuyanov, V. Huguet, M. Parker, R., *ITER Joint Central Team. Nucl. Fusion*, **39** (1999), 1295–1308. https://doi.org/10.1088/0029-5515/39/9y/307

[2] Aymar, R., ITER R&D: Executive Summary: Design Overview, *Fusion Eng. Des.*, **55** (2001), 107–118. https://doi.org/10.1016/s0920-3796(01)00192-2

[3] Bolt, H., Barabash, V., Krauss, W., Linke, J., Neu, R., Suzuki, S., Yoshida, N., Materials for the plasma-facing components of fusion reactors*J. Nucl. Mater.*, **329–333** (2004), part1, 66–73. https://doi.org/10.1016/j.jnucmat.2004.04.005

[4] P. Sigmund, Theory of Sputtering. I. Sputtering Yield of Amorphous and Polycrystalline Targets, *Phys. Rev.*, **184** (1969), 383-416.

[5] R. Behrisch, W. Eckstein, *Sputtering by Particle bombardment: Experiments and Computer Calculations from Threshold Energies*, Springer, Berlin, 2007.

[6] K. Wasa, M. Kitabatake, H. Adachi, *Thin Film Materials Technology-Sputtering of Compound Materials*, William Andrew Publishing/Noyes, 2004, p. 71.

[7] P. Sigmund, *Sputtering by particle bombardment* I, Springer "Sputtering by ion bombardment theoretical concepts", 1981, p. 9.

[8] Z. M. Luo, S. Wang, *Phys*., **74** (1987), 1885.

[9] Z. M. Luo, Q. Hou, Theoretical calculations of energy transfer from noble gases to surfaces, *J. Appl. Phys*. **74** (1993), 6007.

[11] R. Behrisch. *Sputtering by Particle Bombardment I, Topics in Applied Physics*, vol. 47, Springer, Berlin, 1981.

[11] H.H. Andersen and P. Sigmund, Defect distributions in channeling experiments, *Nucl, Instr. and Meth*., **38** (1965), 238-240. https://doi.org/10.1016/0029-554x(65)90144-8

[12] W. Eckstein, J. Bohdansky and J. Roth, Plasma-Material Interaction Data for Fusion, *Suppl. Nucl. Fusion,* **1** (1991), 1-51.

[13] J. Roth, J. Bohdansky and W. Ottenberger, Data on Low Energy Light Ion Sputtering, Max-Planck-Institut fur Plasma physik, IPP Report 9/26, 1979.

[14] L. Zhang, X. Xu, Y. Wu, Sputtering effect of low-energy ions on biological target: The analysis of sputtering product of urea and capsaicin, *Nucl. Instrum. Methods Phys.*, **308** (2013), 28-33. https://doi.org/10.1016/j.nimb.2013.04.053

[15] D.S. Sidorov, N.I. Chkhalo, M.S. Mikhailenko, A.E. Pestov, V.N. Polkovnikov, Sputtering of carbon using hydrogen ion beams with energies of 60–800 eV, *Nucl. Instrum. Methods Phys. Res. B,* **387** (2016), 73-76. https://doi.org/10.1016/j.nimb.2016.10.007

[16] J. Bohdansky, A universal relation for the sputtering yield of monatomic solids at normal ion incidence, *Nucl. Instr. and Meth. B,* **2** (1984), 587-591. https://doi.org/10.1016/0168-583x(84)90271-4

[17] V. I Shulga, Note on the artefacts in SRIM simulation of sputtering, *Appl. Surf. Sci.*, **439** (2018), 456-461. https://doi.org/10.1016/j.apsusc.2018.01.039

Received: August 17, 2019; Published: September 11, 2019